Industrial Engineering Letters
ISSN 2224-6096 (Paper) ISSN 2225-0581 (online)
Vol 2, No.9, 2012

Comparing Chatter Stability of End-Milling Processes of Different Number of Teeth

Ozoegwu Chigbogu Godwin[1*] Ofochebe Sunday Madubueze[1] Oluwadara Benjamin Segun[2] Ezeliora Daniel Chukwueme[3] Ani Moses Chukwuma[4]

[1]Department of Mechanical Engineering, Nnamdi Azikiwe University PMB 5025, Awka
[2]Department of Mechanical Engineering, Ekiti State University, Ado Ekiti
[3]Department of Industrial Production Engineering, Nnamdi Azikiwe University, Awka.
[4]Department of Mechanical Engineering, Federal Polytechnic Oko, Anambra State

Abstract

The cutting forces and dynamic stability of end milling of full radial immersion are compared for end-millers of one to ten teeth. The parameters; tool mass $m = 0.431kg$, tool natural frequency $\omega_n = 5700rads^{-1}$, tool damping ratio $\xi = 0.02$ and feed speed $v = 0.0025ms^{-1}$ are considered fixed for the millers. An end-milling tooth normally has positive rake angle and small cutting edge radius thus workpiece material cutting coefficient $C = 3.5 \times 10^7 Nm^{-7/4}$ is also considered fixed since ploughing effect is not expected to be noticeably affected by change in number of teeth. It is seen that periodic cutting force reduces as the number of teeth increases. A method of milling stability analysis as proposed by Ding et al known as full-discretization is utilized in generating the stability charts. Use is made of the Simpson's rule in establishing for the studied system that chatter stability decreases as the number of teeth increases in the low spindle speed range $(0 - 10000rpm)$ and that lowest chatter stability at high spindle speed range $(10000 - 31000rpm)$ occurs for the five tooth miller. Recommendations are made for the machinist based on these findings. The critical characteristic multipliers at single minimum point of each secondary Hopf bifurcation lobe (SHBL) are postulated to leave the unit circle along imaginary axis when number of teeth of slotting miller is greater than two. This phenomenon is noticed for the one and two tooth millers at two turning points that are not necessarily local minima of each SHBL.

Keywords: Chatter, delay, full-discretization, periodic cutting force, discrete time map, bifurcation

1. Introduction

Chatter is an unstable vibration in machining due regenerative effects that are originally triggered by internal and external perturbations. Regenerative effect is the effect of waviness created on a machined surface due to perturbed dynamic interaction between the tool and the workpiece. In the next tool pass there will be a variation in chip thickness with concomitant cutting force variation causing vibration which subsequently builds up to chatter if cutting parameter combination is unfavourable. Modelling of regenerative vibration normally results in delay-differential equations (DDEs) which is periodic for milling process. Time domain numerical analysis of this equation by Ozoegwu (2012, pp. 43-55) resulted in the

deduction that perturbation history does not affect stability in large as long as cutting parameter combination is stable thus a deterministic or stochastic sequence of perturbations is not expected to affect chatter stability of milling with stable cutting parameter combination. It is then considered a milestone that cutting parameter space of milling can be demarcated as done in this work into stable and unstable subspaces.

The subtleties of milling process are considerably studied. It has been proven both analytically by Insperger & Stepan (2000, pp.119-123) and experimentally by Davies et al (2002, pp.217-225) that milling bifurcation is either of secondary Hopf or flip type. The stability of low radial immersion milling is given detailed study by Davies et al (2002, pp.217-225). Details of development of analytical model of fully-immersed end-milling are presented in this work. End-milling process with the parameters; tool mass $m = 0.431\text{kg}$, tool natural frequency $\omega_n = 5700\text{rads}^{-1}$, tool damping ratio $\xi = 0.02$, workpiece material cutting coefficient $C = 3.5 \times 10^7\text{Nm}^{-7/4}$ and feed speed $\text{v} = 0.0025\text{ms}^{-1}$are inserted into the model at different number of teeth N. The resulting stability charts are validated by numerical simulation of solution of governing DDE by MATLAB dde23. Attention is given to the numerical results to quantify the effect N has on periodic cutting force $F_p(t)$ and chatter stability. It is observed that amplitude and range $F_p(t)$ decrease as N of end miller increases. Effect of N on size of chatter stability of resulting charts is investigated using the Simpson's rule.

Another major contribution of this work is that the stability lobes of the resulting charts are studied by numerical simulation. In the spindle speed range$(100\text{rpm} \leq \Omega \leq 30100\text{rpm})$, secondary Hopf lobes (SHBLs) and flip bifurcation lobes (SHBLs) are seen when $N \leq 3$ while only the former is seen when $N \geq 5$. It is confirmed in another work by Ozoegwu et al (2012) that the result that characteristic multipliers at single minimum point of each SHBL of a slotting three tooth end-miller is pure imaginary. This same result is also seen in this work to be applicable when $N \geq 4$. This same result is discovered here to be applicable at two turning points (not necessarily local minima) of each SHBL when $N = 1$ or 2. The equation postulated by Ozoegwu (2012) to hold for chatter frequencies at minimum point of each SHBL for $N = 3$ is also concluded to hold at the two pure imaginary turning points of each SHBL of $N = 1$ or 2 and those of $N \geq 4$

2. The milling cutting force

A good model for cutting force is needed for successful dynamic modelling of machining. Cutting force is distributed in three dimensions on the active face of the tool having components in the tangential, radial and axial directions of the tool. Obtaining an accurate model for cutting force is impossible not only because it basically has chaotic features but because of the complexities deriving from chip formation effects like friction, heat, plastic flow, mechanical hardening and fracture. This means that the most accurate cutting force model can only result from advanced continuum mechanics. Stepan (1998, pp. 165-192) noted that such complex model would make analytical study of machining stability impossible. Davies et al(1999) pointed out that cutting force models used in machine tool stability analysis are thus based on empirical determination of cutting force coefficients that provide a good approximation of the effects of chip formation process. In these simplistic models, cutting force is no longer distributed but concentrated. A cutting force model found in the work of Stepan et al (2003, pp. 1-2) and credited to the works of Tlusty in

which the component of cutting force in line with prescribed feed F_x has a non-linear empirical form

$$F_x = Cwf_a^{\gamma} \quad (1)$$

is an example of such force model. In (1), C is the cutting force coefficient, w is the depth of cut, f_a is the actual feed rate which is the difference between present and one period delayed position of tool and γ is a less-than-unity exponent that is experimentally determined. γ has a typical value of $3/4$ for the three-quarter rule adopted in this work. Equation (1) is applied directly in dynamic modelling of orthogonal turning process because of time-invariance of chip thickness under unperturbed cutting conditions. In orthogonal cutting process, the cutting edge of the tool is perpendicular to the feed motion as seen in John (1992, p.360). The end-milling system of figure1a in which a machined surface that is at right angle with the cutter axis is produced gives that the tool holder is fixed during milling operation. The spindle is given a rotational speed of Ω rpm while milling feed rate $f = v\tau$ in meters per tool period is imparted on the worktable. v is prescribed feed speed and τ is tool period given as spindle period per teeth for uniformly space teeth. The model being considered is a milling tool of N teeth creating a slot through a workpiece. In end-milling there are added complexities due to multiplicity of tool cutting edge and time-dependence of chip thickness as seen in figure1b.

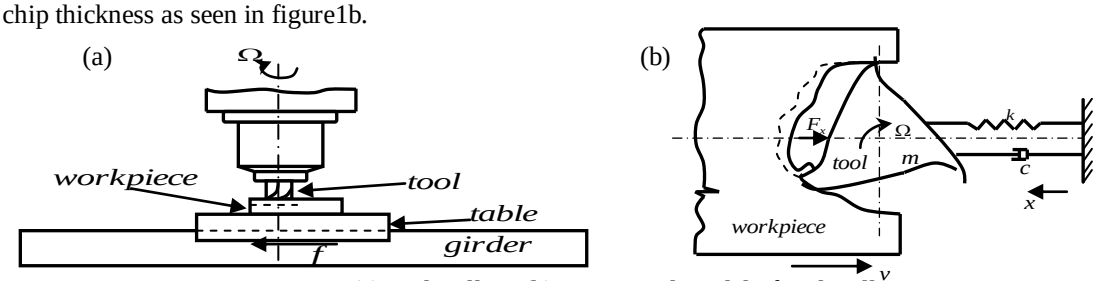

Figure 1. (a) End-milling (b) Dynamical model of end-milling

The x-component of cutting force for the jth tooth of a milling tool is a vector sum of tangential and normal cutting force components $F_{tang,j}(t)$ and $F_{norm,j}(t)$ respectively as shown in a milling tooth-workpiece disposition of figure2. The y-component of cutting force is considered in this work to be of much less dynamic consequence since the tool is constrained from motion in y-direction in slotting operation especially when $N \geq 3$.

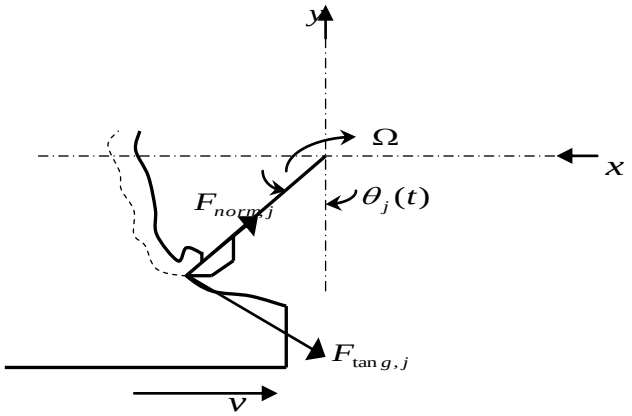

Figure 2. Milling tooth-workpiece disposition

The cutting force law adopted from Insperger (2002) for the jth tooth is $F_{tang,j}(t) = Cw\{f_a sin\theta_j(t)\}^{\gamma}$ and $F_{norm,j}(t) = 0.3F_{tang,j}(t)$ where $\theta_j(t) = (\pi\Omega/30)t + 2\pi(j-1)/N + \alpha$ and $f_a = x(t) -$

$x(t-\tau)$. α is the initial angular position of the tooth with j=1. The $x-$component of cutting force on the tool becomes

$$F_x(t) = wq(t)[x(t) - x(t-\tau)]^{\gamma} \quad (2)$$

where $q(t) = \sum_{j=1}^{N} g_j(t) C sin^{\gamma}\theta_j(t)\left[0.3 sin\theta_j(t) + cos\theta_j(t)\right]$ and screen or switching function $g_j(t)$ takes the values 1 or 0 depending on whether jth tooth is cutting or not. For slotting operation considered as shown in figure1b, the start and end angles will have the values $\theta_s = 0^o$ and $\theta_e = 180^o$. Under this condition it becomes clear from the workpiece-tool disposition of figure2 that $g_j(t) = 0.5\{1 + sgn\sin\theta jt$. In end-milling, cutting edge radius is very small and uncut chip thickness relatively big with it. This means that variation in ploughing effect with variation in number of teeth at fixed tool diameter could be ignored. The implication is that the constants C, γ and 0.3 in the cutting force law are considered fixed for all the tools considered. This assumption is seen implied in the work by Bobrenkov et al (2010, pp. 585–606) in which the same set of parameters are used in the stability analysis of one tooth, four tooth, six tooth and ten tooth millers.

Stationary milling is the needed ideal that can only occur when there is no perturbation. In stationary milling the actual feed f_a becomes equal to the prescribed feed $f = v\tau$ such that (2) becomes

$$F_p(t) = w(v\tau)^{\gamma} q(t) \quad (3)$$

This is the stationary cutting force about which the realistic cutting force of (2) varies. If the milling process is stable, an initially chaotic cutting force will tend to equilibrium (stationary) cutting force as perturbation dies out. Since tool-workpiece disposition repeats after every time $t = \tau = 60/(N\Omega)$ interval, the cutting force of stationary milling as given in (3) is τ-periodic. Under stationary condition the end-milling tool is periodically excited by the periodic force $F_p(t)$. $F_p(t)$ is studied for milling processes with the typical specification; $C = 3.5 \times 10^7 \mathrm{Nm}^{-7/4}$, $\gamma = 0.75$, $v = 0.0025\mathrm{m/s}$, $\Omega = 2000\mathrm{rpm}$ and $w = 0.0015\mathrm{m}$ as adopted from Ozoegwu (2012) for one to ten tooth end-millers and plotted in figure3. The amplitude and range of periodic cutting force designated PCFA and PCFR respectively vary with N as seen in figure3. PCFA and PCFR are plotted against N in figure4. A very important observation from figure4 is that PCFA and PCFR decreases as N of end-miller increases from one to four. Though there is net increase in PCFA and net decrease in PCFR on increase from N=4 to N=10, there is slight fluctuation at every step of N. PCFA could be considered fixed at about 3.1N for $N \geq 4$ while PCFR approaches zero for increasing N beyond 4. This means that if N is infinitely large $F_p(t)$ can be approximated as a constant force. This suggests that milling approaches turning in behaviour as N increases. The deduction from the studied system becomes that tool wear and fatigue of machine tool structure would reduce on increasing N in the range $1 \leq N \leq 4$ while the rate of tool wear and fatigue of machine tool structure is not anticipated to be affected by increase on N beyond 4. Recommendation made from standpoint of stationary cutting force becomes that higher number of teeth is more preferred since tool wear and fatigue of machine tool structure would reduce.

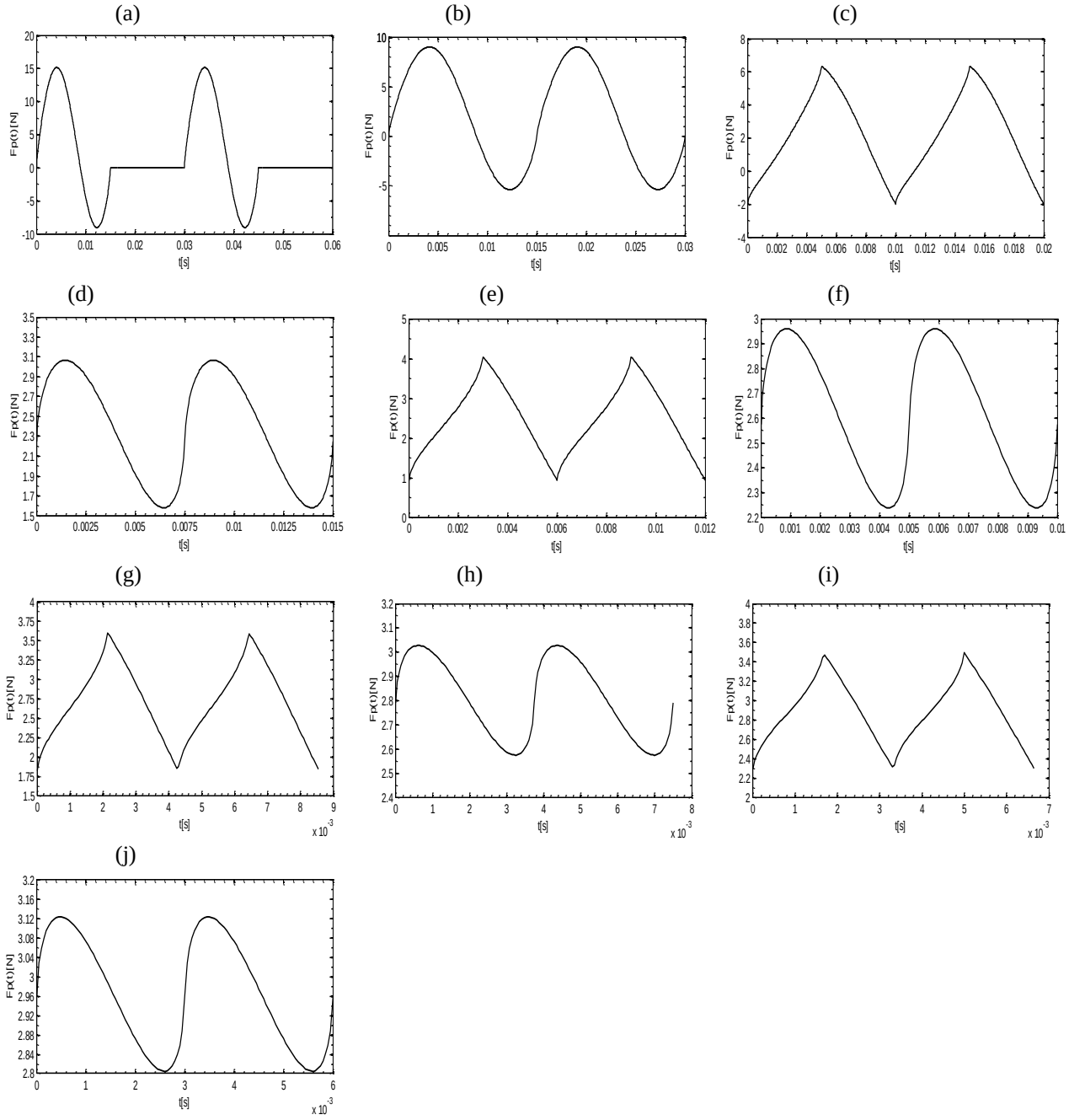

Figure 3: Periodic cutting force of full immersion end-milling for (a) 1 (b) 2 (c) 3 (d) 4 (e) 5 (f) 6 (g) 7 (h) 8 (i) 9 and (j) 10 teeth end-millers.

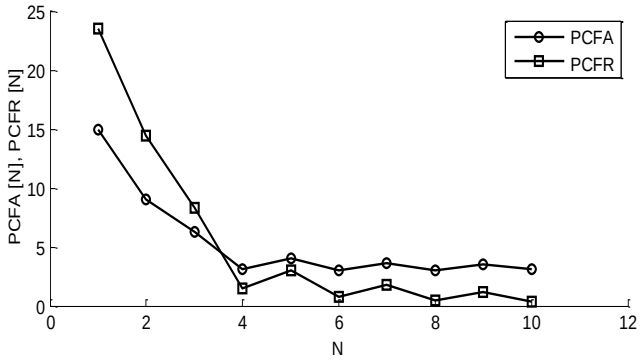

Figure 4. A plot of amplitude of periodic cutting force (PCFA) and Range of periodic cutting force (PCFR)

3. The equation of regenerative vibration for milling process

The parameters of the milling process as depicted on the dynamical model of figure1b are; m mass of tool, c the equivalent viscous damping coefficient modelling the hysteretic damping of the tool system and k the stiffness of the tool. Figure1b is a single degree of freedom vibration model of a slotting end-milling tool. Single degree of freedom model is considered because most encountered resonance in machining involves the fundamental natural frequency especially when it is far separated from higher frequencies. This is based on the works by Stepan (1998, p. 165-192) and by Stepan and Kalmar-Nagy (1997). Also majority the tools (especially the ones with more than three teeth) are considered in this work to be constrained to vibrate predominantly in the feed direction under full-immersion. The wavy regenerative machined surface that sustains chatter vibration is shown enlarged on figure1b. The differential equation governing the motion of the tool as seen from figure1b is as given in (4)

$$m\ddot{x}(t) + c[\dot{x}(t) - vt] + k[x(t) - vt] + F_x = 0 \quad (4)$$

The compact notations; $x(t) = x$ and $x(t-\tau) = x_\tau$ are hence used. The motion of the tool is modeled by Insperger (2002) to be a linear superposition of prescribed feed motion vt, tool response to τ -periodic force $F_p(t)$ of non-perturbed tool-workpiece interaction $x_t(t)$ and perturbation $z(t)$ such that

$$x(t) = vt + x_t(t) + z(t) \quad (5)$$

In light of the fact that $x_\tau = v \times (t-\tau) + x_t(t-\tau) + z_\tau$ and $x_t(t) = x_t(t-\tau)$, substitution of (5) into (4) gives

$$m\ddot{x}_t + c\dot{x}_t + kx_t + m\ddot{z} + c\dot{z} + kz = -q(t)w[v\tau + (z - z_\tau)]^\gamma \quad (6)$$

Without perturbation (that is $z = z_\tau = 0$), (6) simplifies to

$$m\ddot{x}_t + c\dot{x}_t + kx_t = -F_p(t) \quad (7)$$

It is seen from (7) that τ-periodic tool response $x_t(t)$ is a steady state response driven by $-F_p(t)$. The trajectory of tool periodic motion can be estimated via harmonic or Fourier series analysis in which motion is calculated as a linear superposition of tool response to individual harmonics of excitation $-F_p(t)$. This is not done here due to lack of space albeit such analysis is necessary because some very productive cutting parameter combination that are chatter free will highly intensify the amplitude of $x_t(t)$ and facilitate tool and machine structural fatigue and wear. This effect will be worst felt under resonant conditions. Equation (7) means that (6) becomes

$$m\ddot{z} + c\dot{z} + kz = F_p(t) - (v\tau)^{-\gamma}F_p(t)[v\tau + (z - z_\tau)]^\gamma \tag{8}$$

Linearized Taylor series of (8) reads

$$m\ddot{z} + c\dot{z} + kz = -\gamma(v\tau)^{-1}F_p(t)(z - z_\tau) \tag{9}$$

Equation (9) put in modal form becomes

$$\ddot{z} + 2\xi\omega_n\dot{z} + \left[\omega_n^2 + \frac{wh(t)}{m}\right]z = \frac{wh(t)}{m}z_\tau \tag{10}$$

Where the specific force variation $h(t) = \gamma(v\tau)^{\gamma-1}q(t)$ could be seen to have the same period and shape or profile but not amplitude or range as $F_p(t)$. With the substitutions $y_1 = z$ and $y_2 = \dot{z}$ made, (10) could be put in state differential equation form as

$$\dot{\boldsymbol{y}} = \boldsymbol{A}\boldsymbol{y} + \boldsymbol{B}(t)\boldsymbol{y} - \boldsymbol{B}(t)\boldsymbol{y}_\tau \tag{11}$$

where $\dot{\boldsymbol{y}} = \begin{Bmatrix}\dot{y}_1\\ \dot{y}_2\end{Bmatrix}$, $\boldsymbol{y}_\tau = \begin{Bmatrix}y_{1,\tau}\\ y_{2,\tau}\end{Bmatrix}$, $\boldsymbol{A} = \begin{bmatrix}0 & 1\\ -\omega_n^2 & -2\xi\omega_n\end{bmatrix}$ and $\boldsymbol{B}(t) = \begin{bmatrix}0 & 0\\ -\frac{wh(t)}{m} & 0\end{bmatrix}$. The natural frequency and damping ratio of the tool system are given in terms of modal parameters k, m and c respectively as $\omega_n = (k/m)^{1/2}$ and $\xi = c/2(mk)^{1/2}$. These modal parameters could easily be extracted from experimental plot of the tool frequency response function $R(\omega) = X/F = 1/[(k - \omega^2 m)^2 + \omega^2 c^2]^{1/2}$ for forced single degree of freedom vibration. Either of the equations (10 or 11) is the general linear periodic delay-differential equation model for milling process with single discrete delay.

4. Chatter stability analysis via full-discretization method

A method of full-discretization is first developed by Ding et al (2010, pp.502–509) for study of milling stability. The method of full-discretization is compared with the method of semi-discretization by Insperger (2010, pp.658–662). The method of full-discretization is based on a $2(k+1)$-dimensional discrete time map of (11) which reads

$$\boldsymbol{x}_k = \boldsymbol{D}_{k-1} \dots\dots \boldsymbol{D}_0\boldsymbol{x}_0 \tag{12}$$

with

$$\boldsymbol{D}_i = \begin{bmatrix}\boldsymbol{D}_{11}^i & \boldsymbol{0} & \cdots & \boldsymbol{0} & \boldsymbol{D}_{1k}^i & \boldsymbol{D}_{1,k+1}^i\\ \boldsymbol{I} & \boldsymbol{0} & \cdots & \boldsymbol{0} & \boldsymbol{0} & \boldsymbol{0}\\ \boldsymbol{0} & \boldsymbol{I} & \cdots & \boldsymbol{0} & \boldsymbol{0} & \boldsymbol{0}\\ \vdots & \vdots & \vdots & \vdots & \vdots & \vdots\\ \boldsymbol{0} & \boldsymbol{0} & \boldsymbol{0} & \boldsymbol{0} & \boldsymbol{I} & \boldsymbol{0}\end{bmatrix} \tag{13}$$

$$\boldsymbol{x}_i = \{\boldsymbol{y}_i \quad \boldsymbol{y}_{i-1} \quad \boldsymbol{y}_{i-2} \quad \cdots \quad \boldsymbol{y}_{i-k}\}^T \tag{14}$$

where $= 0, 1, 2, \dots\dots\dots (k-1)$, $\boldsymbol{D}_{11}^i = (\boldsymbol{I} - \boldsymbol{F}_{i+1})^{-1}(e^{\boldsymbol{A}\Delta t} + \boldsymbol{F}_i)$, $\boldsymbol{D}_{1r}^i = -(\boldsymbol{I} - \boldsymbol{F}_{i+1})^{-1}\boldsymbol{F}_{i+1}$, $\boldsymbol{D}_{1,r+1}^i = -(\boldsymbol{I} - \boldsymbol{F}_{i+1})^{-1}\boldsymbol{F}_i$, $\begin{matrix}\boldsymbol{F}_i = \left(\frac{1}{\Delta t}\boldsymbol{\Phi}_0 - \frac{2}{\Delta t}\boldsymbol{\Phi}_1 + \frac{1}{\Delta t^2}\boldsymbol{\Phi}_2\right)\boldsymbol{B}_i + \left(\frac{1}{\Delta t}\boldsymbol{\Phi}_1 - \frac{1}{\Delta t^2}\boldsymbol{\Phi}_2\right)\boldsymbol{B}_{i+1}\\ \boldsymbol{F}_{i+1} = \left(\frac{1}{\Delta t}\boldsymbol{\Phi}_1 - \frac{1}{\Delta t^2}\boldsymbol{\Phi}_2\right)\boldsymbol{B}_i + \left(\frac{1}{\Delta t^2}\boldsymbol{\Phi}_2\right)\boldsymbol{B}_{i+1}\end{matrix}$, $\boldsymbol{\Phi}_0 = \boldsymbol{A}^{-1}(e^{\boldsymbol{A}\Delta t} - \boldsymbol{I})$,

$\boldsymbol{\Phi}_1 = \boldsymbol{A}^{-1}(\boldsymbol{\Phi}_0 - \Delta t\boldsymbol{I})$, $\boldsymbol{\Phi}_2 = \boldsymbol{A}^{-1}(2\boldsymbol{\Phi}_1 - (\Delta t)^2\boldsymbol{I})$

Equation (12) is obtained by dividing the discrete delay τ of the system into k equal time intervals $[t_i, t_{i+1}]$ and approximating (11) as

$$\dot{\boldsymbol{y}} = \boldsymbol{A}\boldsymbol{y} + \widetilde{\boldsymbol{B}}(t)\widetilde{\boldsymbol{y}} - \widetilde{\boldsymbol{B}}(t)\widetilde{\boldsymbol{y}}_\tau, \qquad t \in [t_i, t_{i+1}] \tag{15}$$

where $t_i = i\frac{\tau}{k} = i\Delta t$, $\widetilde{\boldsymbol{B}}(t) = \boldsymbol{B}_i + \frac{\boldsymbol{B}_{i+1}-\boldsymbol{B}_i}{\Delta t}(t-t_i)$, $\widetilde{\boldsymbol{y}}(t) = \boldsymbol{y}_i + \frac{\boldsymbol{y}_{i+1}-\boldsymbol{y}_i}{\Delta t}(t-t_i)$ and $\widetilde{\boldsymbol{y}}_\tau(t) = \boldsymbol{y}_{i-k} + \frac{\boldsymbol{y}_{i+1-k}-\boldsymbol{y}_{i-k}}{\Delta t}(t-t_i)$. It should be understood that $\boldsymbol{B}_i$ equals $\boldsymbol{B}(t_i)$**.** Equation (15) is solved as an ordinary differential equation and coupled for all discrete intervals to give discrete time map (12) with the monodromy operator $\boldsymbol{\Phi} = \boldsymbol{D}_{k-1} \ldots \ldots \boldsymbol{D}_0$ acting as a linear operator that transforms the delayed state $\boldsymbol{x}_0$ to the present state $\boldsymbol{x}_k$. The necessary and sufficient condition for asymptotic stability of the system is that all the eigen-values of the matrix $\boldsymbol{\Phi}$ must exist within a unit circle centred at the origin of the complex plane. The magnitude of the eigen-values depends on the cutting parameter combination thus stability transition curve along which the maximum magnitude characteristic multipliers lie on the unit circle is tracked to demarcate stable from unstable sub domains. These critical eigenvalues are analytically established for milling process by Insperger & Stepan (2000, pp.119-123) and experimentally established by for milling process by Davies et al (2002, pp.217-225) to be either -1 (in the case of flip or period two bifurcation) or a complex conjugate pair (in the case of secondary Hopf or Neimark-sacker bifurcation).

5. Results and discussions

Making use of $k = 70$ in eigen-value analysis of $\boldsymbol{\Phi}$ for end-milling systems with the following parameters; $m = 0.431\text{kg}, \omega_n = 5700\text{rads}^{-1}$, $\xi = 0.02$, $C = 3.5 \times 10^7 \text{Nm}^{-7/4}$ and $\text{v} = 0.0025\text{ms}^{-1}$, results in the stability transition curves of figure5. Figures5a to 5j are for one to ten tooth end-milling respectively. The light sub area is for stable operations while the dark sub area is for unstable operation. Periodic cutting force will act as an attractor to initially perturbed cutting force as time progresses at any operation in the stable sub area. The uniqueness of each stability chart means that N has considerable effect on chatter stability of full-immersion end-milling. In order to quantify this effect, numerical integration method of Simpson's rule is used to get an estimate of the stable areas of the charts. This result is summarized in figure6 in which the stable area of the low spindle speed range $(0-10000\text{rpm})$ designated A_l (but as Al in fig. 6), the stable area of the high spindle speed range $(10000-31000\text{rpm})$ designated A_h (but as Ah in fig. 6) and total stable area of spindle speed range $(100-31000\text{rpm})$ designated A_t (but as At in fig. 6) are plotted against N. It is seen that stability decreases as N increases in the low spindle speed range being that A_l has the biggest value at $N = 1$ and the lowest value at $N = 10$. It is seen from the variation of A_h with N that lowest chatter stability of slotting at high spindle speed occurs at $N = 5$. It is also seen from variation of A_t that minimum overall stability occurs at $N = 5$. The areas A_h and A_t follow similar trends approaching each other as N increases towards 10. This means chatter stability of low spindle speed range is least at $N = 10$. Mathematical validity of the stability charts of figure5 is based on numerical simulation using MATLAB dde23 in which graphical solutions of (11) are generated at chosen cutting parameter points of the charts. For example, results of such numerical simulation at $\Omega = 12000\text{rpm}$ and $w = 1.5\text{mm}$ for one tooth miller and $\Omega = 6000\text{rpm}$ and $w = 1\text{mm}$ for six tooth miller are shown in figure7. The history used is $y_1 = 0.0000001\text{m}$ and y_2=0.000001m/s for $t\epsilon[-\tau, 0]$. Slot end-milling of one tooth miller at $\Omega = 12000\text{rpm}$ and $w = 1.5\text{mm}$ is seen from figure7.a to be a stable operation in which perturbation asymptotically approaches zero in large. Solution at $\Omega = 6000\text{rpm}$ and $w = 1\text{mm}$ for six tooth miller as shown in figure7.b is unstable being that perturbation grows with time. The stability chart of the three tooth end-miller is seen in the work by Ozoegwu (2012) to be given detailed simulated validation. This is shown in figure8.

The nature of bifurcation occurring at different portions of the stability transition curve is determined by insertion of critical parameter combinations into $\boldsymbol{\Phi}$ and extracting the critical characteristic multipliers.

Both secondary Hopf bifurcation lobes (SHBLs) and flip bifurcation lobes (FBLs) are seen in the transition curves of the fully-immersed one, two and three tooth end-milling in the spindle speed range $(100\text{rpm} \leq \Omega \leq 30100\text{rpm})$ considered. Any two nearest downward arrow encloses bifurcation lobe of either secondary Hopf type (indicated with H) or flip type (indicated with F). FBL is not seen for higher number of teeth in this Ω range. Stability charts for $N \geq 3$ exhibit SHBLs with one local minimum each while one and two tooth charts exhibit SHBLs that has more than one local minimum. A discovery on stability chart of slotting three tooth end-miller that critical characteristic multipliers are almost pure imaginary at the minimum points of SHBLs and get closer to the negative real axis when critical spindle speed increases from the minimum points is already made by Ozoegwu et al (2012). An equation

$$\omega_{\text{shm}} = \frac{N\pi\Omega}{120}[\pm n + 4k],\ n = 1, 3, 5 \ldots . and\ k = \cdots -2, -1, 0, 1, 2, \ldots . \tag{23}$$

that governs the infinitely many but discrete secondary Hopf bifurcation chatter frequencies at minimum points of SHBLs of three tooth miller is also postulated by Ozoegwu et al (2012). This equation is confirmed in this work to be applicable at minimum points of slotting when $N \geq 4$ but not when $N = 1$ or 2 since investigation of SHBLs enclosed within the downward arrows connected by horizontal lines (see figure 6a and b) shows that this equation can only be applicable at points marked by inclined arrows. These points are two for $N = 1$ or 2 and are not necessarily local minima thus these SHBLs differs from those of $N \geq 3$ in a fundamental way. What looks like jagged edges of hack saw occurs in the high spindle speed range when $N \geq 5$ could be as a result of low tool damping. The calculated characteristic multipliers at the critical parameter combinations (25000rpm, 0.001m), (27000rpm, 0.001m) and (29000rpm, 0.0014m) of five tooth miller are -0.9741 + 0.0940i, -1.0150 and -1.0001 respectively. This suggests that flip bifurcation starts to occur at $\Omega = 25000\text{rpm}$. At this point there is a physical change in the stability transition curve. Characteristic multipliers calculated on the jagged edges when $N \geq 6$ indicates both flip and secondary Hopf bifurcations though there is rising preponderance of flip eigen-values and decrease in the size of imaginary part of secondary Hopf eigen-values as Ω increases in the jagged domain. This means that the jagged domains are extensions of SHBLs to which they are attached though vertical lines are used in figures5e to 5j to mark the spindle speed range in which SHBL are obviously seen. The only major physical difference between tools with $N \geq 3$ and the ones with $N = 1$ or 2 is simultaneous teeth engagement that occurs when $N \geq 3$. This is considered to be a contributor of the observed differences in SHBLs of tools with $N \geq 3$ and the ones with $N = 1$ or 2

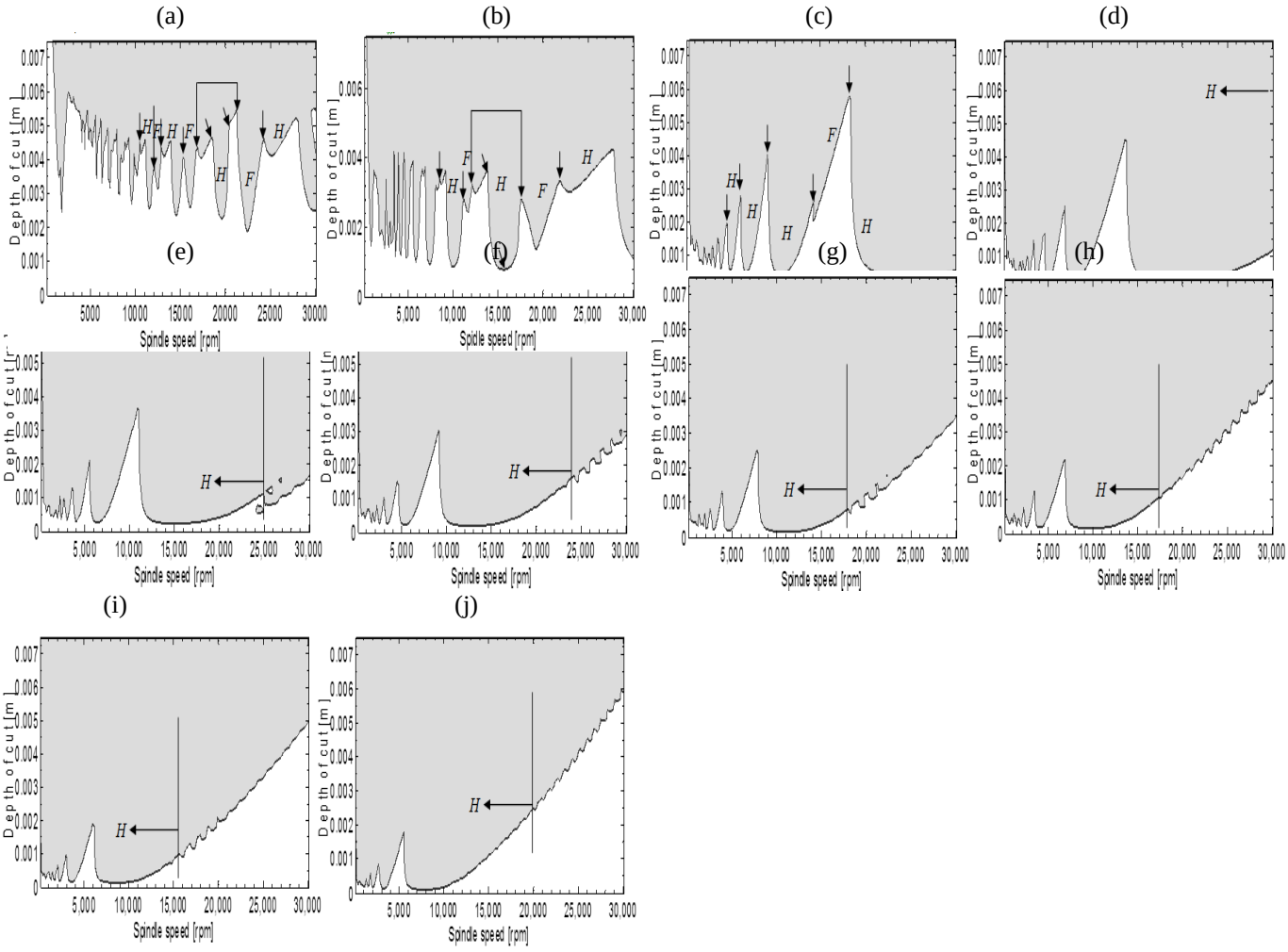

Figure 5. Stability charts at full-immersion on $(\Omega - w)$ space with light stable sub-domains and dark unstable sub-domains for (a) 1 (b) 2 (c) 3 (d) 4 (e) 5 (f) 6 (g) 7 (h) 8 (i) 9 and (j) 10 teeth end-millers.

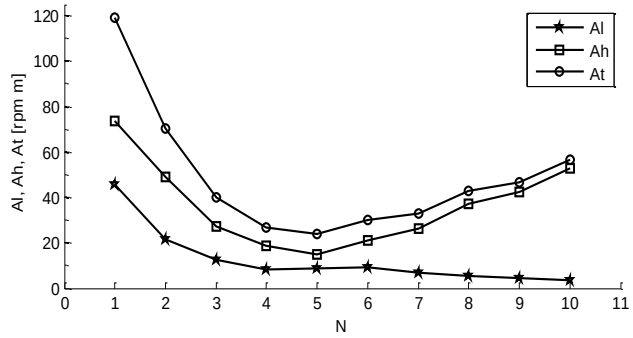

Figure 6. Stable areas of the charts against N. A_l is stable area of low-speed range, A_h is stable area of high-speed range and A_t is total stable area

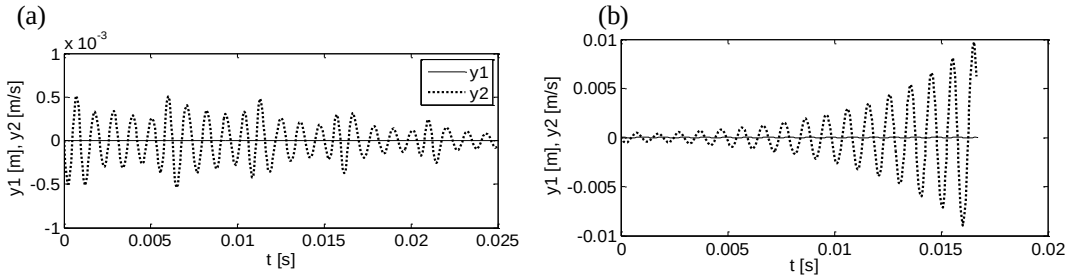

Figure 7. Tool response at (a) $\Omega = 12000\text{rpm}$ and $w = 1.5\text{mm}$ for 1 tooth miller is stable, (b) $\Omega = 6000\text{rpm}$ and $w = 1\text{mm}$ for 6 tooth miller is unstable.

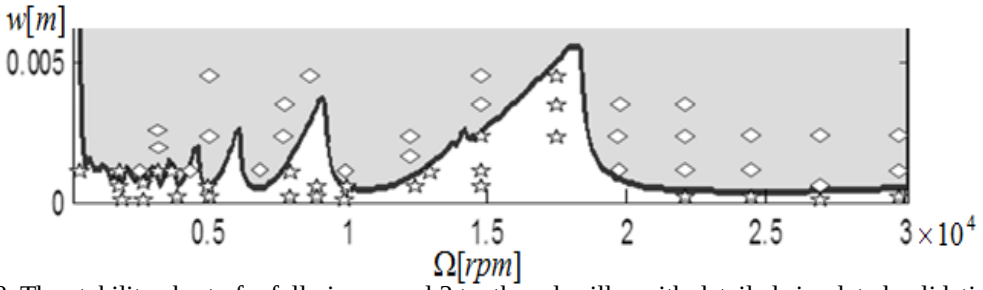

Figure 8. The stability chart of a fully immersed 3 tooth end-miller with detailed simulated validation. Stars are for stable where diamonds are for unstable MATLAB dde23 solutions.

6. Conclusion

The stationary cutting forces of slotting one to ten tooth end-millers are compared. It is observed that amplitude and range of stationary cutting force decrease as the number of teeth of end miller increases. Recommendation is then made that higher number of teeth should be more preferred if tool wear and fatigue of machine tool structure are of highest priority.

Stability analysis of end-milling on parameter plane of spindle speed and depth of cut using full-discretization method as proposed by Ding et al results in the generation of stability charts for one to ten tooth end-millers with parameters; $m = 0.431kg$, $\omega_n = 5700rads^{-1}$, $\xi = 0.02$, $C = 3.5 \times 10^7\text{Nm}^{-7/4}$ and $\text{v} = 0.0025\text{ms}^{-1}$. The stability of the low spindle speed range $(0 - 10000rpm)$ decreases as the number of teeth increases. Lowest chatter stability of slotting at high spindle speed range $(10000 - 31000rpm)$ occurs for the five tooth miller. Minimum overall stability also occurs for the five tooth miller in the overall spindle speed range $(100 - 31000\text{rpm})$ considered .The recommendation becomes that an operator of a low speed end-milling machine tool should go for tools with number of teeth less than three if component dimensional integrity and accuracy are of highest priority. If the machine operates in the high speed range three to seven tooth end-miller should be avoided. Though recommendations based on periodic cutting force and chatter stability partly contradict each other for high speed operation a productive and economic compromise can be reached when equipped with these charts such that productive depth of cut is milled at relatively low stationary cutting force.

It is seen that each secondary Hopf bifurcation lobe of full-immersion end-milling has one local minimum when the number of teeth is above three. A discovery made in another work for a three tooth miller that

critical characteristic multipliers are almost pure imaginary at the minimum point of each secondary Hopf bifurcation lobe and get closer to the negative real axis when critical spindle speed increases from the minimum point is seen in this work to be applicable for higher number of teeth. It is seen that pure imaginary critical characteristic multipliers occur at two distinct turning points that are not necessarily local minima when the number of teeth is one or two.

References

Bobrenkov, O. A., Khasawneh, F. A., Butcher, E. A., & Mann, B. P. (2010). Analysis of milling dynamics for simultaneously engaged cutting teeth. *Journal of Sound and Vibration*, 329, 585–606.

Davies, M. A., Pratt, J. R, Dutterer, B., & Burns, T. J. (2002). Stability prediction for low radial immersion milling. *Journal of Manufacturing Science and Engineering*, 124, 217-225.

Davies, M.A., Burns, T. J. & Schmitz, T. L. (1999). *High-Speed Machining Processes: Dynamics of Multiple Scales.* National Institute of Standards and Technology 100 Bureau Drive, Gaithersburg MD 20899, USA, 1999.

Ding, Y., Zhu, L.M.,. Zhang, X.J., & Ding, H. (2010). A full-discretization method for prediction of milling stability, *International Journal of Machine Tools and Manufacture*, 50, 502–509.

Insperger, T. (2010). Full-discretization and semi-discretization for milling stability prediction: Some comments. *International Journal of Machine Tools and Manufacture*, 50, 658–662.

Insperger, T. (2002). *Stability Analysis of Periodic Delay-Differential Equations Modelling Machine Tool Chatter.* PhD dissertation, Budapest University of Technology and Economics.

Insperger, T., & Stepan, G. (2000). *Stability of High-Speed Milling.* Proceedings of Symposium on Nonlinear Dynamics and Stochastic Mechanics, Orlando, Florida, AMD-24, **1**119-123.

John, V. (1992). *Introduction to Engineering Materials*(3rd ed.). Hampshire: Palgrave, 360.

Ozoegwu, C. G. (2012) *Chatter of Plastic Milling CNC Machine.* M. Eng thesis, Nnamdi Azikiwe University Awka.

Ozoegwu, C. G., Uzoh, C. F., Chukwuneke, J. L., & Okolie P. C. (2012). Chatter stability characterization of a three-flute end-miller using the method of full-discretization. *International Journal of Mechanics and Applications*, In press.

Stepan, G. (1998) *Delay-differential Equation Models for Machine Tool Chatter*: in *Nonlinear Dynamics of Material Processing and Manufacturing*, edited by F. C. Moon, New York: John Wiley & Sons, 165-192.

Stép án, G., Szalai, R., & Insperger, T. (2003) *Nonlinear Dynamics of High-Speed Milling Subjected to Regenerative Effect:* to appear in the book *Nonlinear Dynamics of Production Systems* edited by Gunther Radons, New York: Wiley-VCH, 1-2.

Stepan, G., Kalmar-Nagy, T. (1997) *Nonlinear Regenerative Machine Tool Vibrations.* Proceedings of DETC'97 1997 ASME Design Engineering Technical Conferences, Sacramento, California September 14-17.